Synthesis and molecular structure of a spheroidal binary nanoscale copper sulfide cluster†

Sebastian Bestgen,*[a] Olaf Fuhr,[b,c] Peter W. Roesky[a] and Dieter Fenske*[a,b,c]

The reaction of copper(4-(*tert*-butyl)phenyl)methanethiolate [$CuSCH_2C_6H_4{}^tBu$] with bis(trimethylsilyl)sulfide $S(SiMe_3)_2$ in the presence of triphenylphosphine PPh_3 afforded the binary 52 nuclear copper cluster $[Cu_{52}S_{12}(SCH_2C_6H_4{}^tBu)_{28}(PPh_3)_8]$. The molecular structure of this intensely red coloured nanoscale Cu_2S mimic was established by single crystal X-ray diffraction.

The synthesis of metal-rich coinage metal chalcogenide clusters is of particular interest because these nanoparticulate compounds can act as model systems for the investigation of quantum-confinement effects *e.g.* size-dependent photophysical properties.[1] However, the isolation of such compounds requires an effective shielding of the inorganic cluster core as chalcogenide clusters are thermodynamically unstable towards the formation of bulk M_2E (M = Cu, Ag, Au; E = S, Se, Te).[2] Hence, appropriate ligands which bind to the surface of the cluster are necessary to prevent the formation of *e.g.* copper sulphide. The synthesis of chalcogenide clusters is often achieved by the reaction of a suitable metal salt (*e.g.* CuOAc) and a silylated chalcogenide source (*e.g.* $RESiMe_3$ or $E(SiMe_3)_2$; R = organic group, E = S, Se, Te) in the presence of mono- or bidentate phosphine ligands.[3] The driving force of this reaction is the formation of a Si–OAc bond. Alternatively, also coinage metal thiolates M(SR) (R = organic group; M = Cu, Ag, Au) can be applied together with phosphines and chalcogenide sources to obtain very large molecules.[2a,4] In this type of reaction, the phosphines first break up the oligo- or polymeric network of the insoluble metal thiolate forming different oligonuclear species.[5] These soluble complexes then further react with the silylated chalcogenide source building larger cluster species. Finally, one defined species is obtained by crystallization as a phase pure single crystalline material. Although the crystallization and isolation of one discrete molecule depends very sensitively on the reaction conditions (amount and kind of solvent, phosphine, and ligand, stoichiometry), the products often can be obtained reproducibly and in good yields once those conditions were established and optimized. If such cluster molecules are obtained as single crystalline material, their structure is deducible from single crystal X-ray structural analysis. However, the data collection, solution and refinement is not trivial as these spherical molecules often show rotational disorder, twinning and generally weak scattering at diffraction angles higher than 40° in 2Θ (for MoK_α) or 80° in 2Θ (for CuK_α). Hence, the lack of long-range order in the crystal exacerbates a full structural analysis.[2a]

Herein, we report the synthesis and full characterization of a 52 nuclear binary copper sulfide nanoparticle with a spheroidal shape. For an effective coating of the desired Cu_2S nanoparticles and for an enhanced solubility of the cluster molecules, we chose (4-(*tert*-butyl)phenyl)methanethiol as bulky organic ligand. Following known procedures,[6] $CuSO_4{\cdot}5H_2O$ was reduced to Cu(I) with hydroxylamine hydrochloride ($NH_2OH{\cdot}HCl$) in ammonia as reducing agent. The thus obtained intermediate was subsequently reacted with the thiol giving the copper thiolate complex [$CuSCH_2C_6H_4{}^tBu$] as a brown solid. [$CuSCH_2C_6H_4{}^tBu$] was further reacted with PPh_3 and $S(SiMe_3)_2$ in toluene (Scheme 1). Upon addition of $S(SiMe_3)_2$, the initially cloudy suspension became clear and a

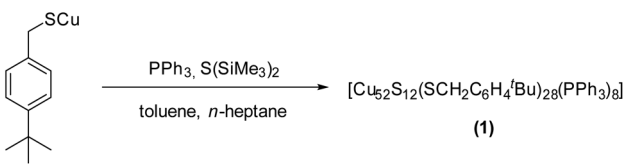

Scheme 1 Synthesis of $[Cu_{52}S_{12}(SCH_2C_6H_4{}^tBu)_{28}(PPh_3)_8]$ (**1**).

[a]*Institute of Inorganic Chemistry, Karlsruhe Institute of Technology (KIT), Engesserstraße 15, 76131 Karlsruhe, Germany. E-mail: sebastian.bestgen@kit.edu, dieter.fenske@kit.edu*

[b]*Institute of Nanotechnology and Karlsruhe Nano Micro Facility (KNMF), Karlsruhe Institute of Technology (KIT), Hermann-von-Helmholtz-Platz 1, 76344 Eggenstein-Leopoldshafen, 76021 Karlsruhe, Germany*

[c]*Lehn-Institute for Functional Materials, School of Chemistry and Chemical Engineering, Sun Yat-Sen University, Guangzhou, China*

gradual colour change from yellow to dark red was observed within approximately 2–3 hours. Removal of toluene and subsequent extraction of the residue with *n*-heptane followed by filtration afforded an intensely red colored solution. Within a few days, the formation of dark red, block-shaped crystals was observed. A facile separation of these crystals by decantation from the mother liquor was possible. The cluster was obtained fully reproducibly in approximately 30% yield (based on $S(SiMe_3)_2$ as limiting reagent).‡

Compound **1** crystallizes in the monoclinic space group *C*2/*c* with half of a molecule in the asymmetric unit. A crystallographic twofold axis is observed through the molecule. Within the unit cell, ten molecules of *n*-heptane (partly disordered) were located and refined. The collected data set was of high quality and thus, all atoms including carbon atoms were anisotropically refined. Compound **1** consist of a $(Cu_2S)_{12}$ core, which is surrounded by eight PPh_3 ligands as well as 28 $[CuSCH_2C_6H_4{}^tBu]$ subunits. The cluster is thus best described as $(Cu_2S)_{12}@[(CuSCH_2C_6H_4{}^tBu)_{28}(PPh_3)_8]$, with all copper atoms in oxidation state +I (Fig. 1).

Within the cluster scaffold, copper ions are coordinated in a distorted linear or trigonal planar fashion, which is quite similar to the coordination modes in chalcocite Cu_2S.[7] Thereby, the thiolates (S1–S14) and the sulfide ions (S15–S20) act as bridging ligands and coordinate to the metal ions in a μ_2-, μ_3- and $\mu_{>3}$-fashion. As expected, Cu–S bond lengths depend on the coordination mode. For μ_2-S1, Cu–S bond lengths of 2.259 Å and 2.293 Å are found. S2–S14 act as μ_3-ligands with av. bond lengths of 2.303 Å. Higher bridging modes up to μ_6 are found for the sulfide ions S^2 S15–S20 with nearly similar Cu–S-distances of av. 2.288 Å. Not surprisingly, sulfide ions are exclusively located within the cluster core (Fig. 2, top and S4†). The phosphine ligands are located at the edges of the cluster (Fig. 1) with Cu–P bond lengths of av. 2.238 Å, which is in the expected range for copper phosphine complexes.[5b,8] In the central copper sublattice, most of the Cu–Cu contacts range between 2.576 Å and 2.984 Å (mean 2.746 Å). Although these values are well below the sum of van der Waals radii for Cu (2.80 Å), previous theoretical investigations exclude significant metallophilic d^{10}–d^{10} interactions.[9] In the center of the cluster, a $Cu_{14}S_8$ unit is observed, in which the copper atoms are arranged in a face centered cubic fashion (fcc) (Fig. 2, bottom).

By considering the extended solid-state structure of **1**, the cluster molecules are arranged in a distorted hexagonal close packing (hcp) (Fig. S3†). Taking the ligand shell into account, the dimensions of the spheroidal cluster are about 3 nm × 2.2 nm, whereas the inorganic core has a block-like structure

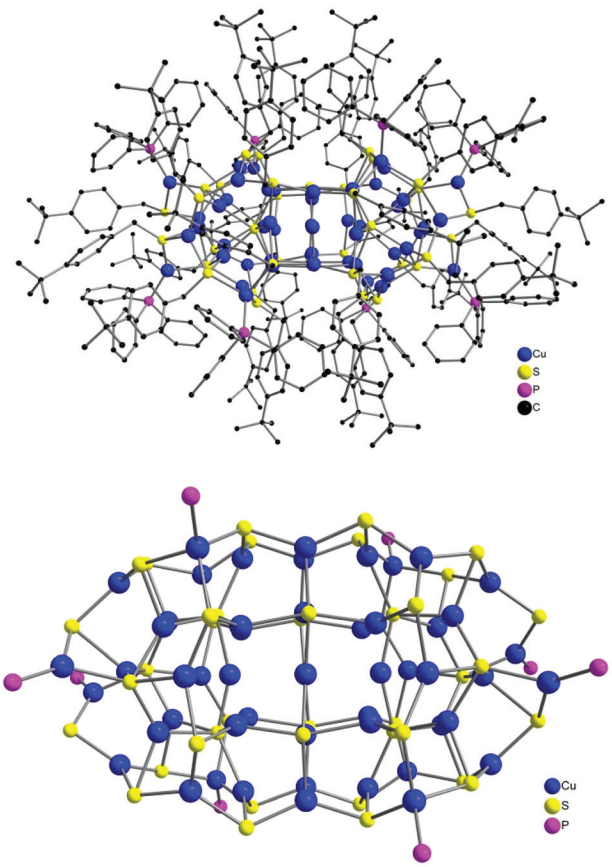

Fig. 1 Top: Molecular structure of $[Cu_{52}S_{12}(SCH_2C_6H_4{}^tBu)_{28}(PPh_3)_8]$ (**1**) in solid state. Bottom: Structure of the inorganic cluster core.

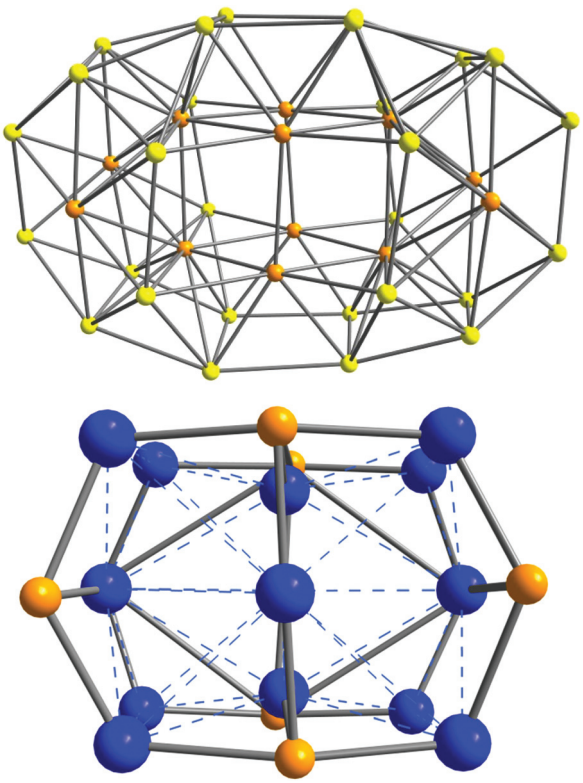

Fig. 2 Top: Sulfur-sublattice with RS^- (yellow) and S^{2-} (orange) in **1**. Bottom: $Cu_{14}S_8$-unit elucidating the distorted fcc arrangement of Cu atoms (blue) inside the cluster core. Lines between S atoms and between Cu atoms are nonbinding and solely illustrate the geometric arrangement.

with a size of approx. 1.6 nm × 0.8 nm × 0.7 nm. To the best of our knowledge, **1** is the second largest spheroidal binary copper sulfide nanocluster ever reported. Despite its unexpectedly low solubility, compound **1** was also investigated by NMR spectroscopy. Unfortunately, only broad and poorly structured resonances were detected in ^{1}H and $^{31}P\{^{1}H\}$ NMR spectra. In the ^{1}H NMR spectrum resonances between 0.7 ppm and 1.6 ppm were observed indicating the presence of *tert*-butyl groups of the thiolate ligand. In the region between 2.8 ppm and 4.8 ppm, multiple resonances were seen, which originate from the SCH_2-moiety of the ligand. Between 6 ppm and 7.8 ppm, a broad signal was observed, which arises both from the phosphine and the thiolate ligands. Within the margin of error for broadened spectra, the integration ratios in the ^{1}H NMR fit well with the composition of **1** deduced from X-ray analysis. In the $^{31}P\{^{1}H\}$ NMR spectrum, broad resonances at −11.6 ppm and −5 ppm were observed, which indicates triphenylphosphine ligands coordinated to copper as well as partially uncoordinated phosphines. Although it is known that some ligands at a cluster surface are mobile with respect to rearrangement and dissociation processes, the broadened nature of the spectra impedes a detailed analysis. As the full coverage of the cluster surface is of crucial importance for their stability, the clusters may either rearrange in an inter- or intramolecular fashion or slowly decompose upon ligand dissociation.[10] This assumption is supported by the observation of a brown insoluble precipitate in the NMR tubes after a few days.

The composition of the obtained crystalline material of **1** was further confirmed by elemental analysis. IR spectra were conducted showing absorption bands at similar wavenumbers as seen in [CuSCH$_2$C$_6$H$_4$^{t}Bu] (Fig. S2†). The purity of the bulk phase was verified by powder X-ray diffraction. The experimental diffraction pattern was compared with the simulated one (based on the single crystal data;§ Fig. S5†). Unfortunately, mass spectrometric investigations by electrospray ionization (ESI-MS) were not successful showing only peaks at mass-to-charge rations between 500 and 1500 (both in the cationic and anionic mode), which correspond to smaller copper thiolate fragments thus indicating decomposition of **1** under ESI-MS conditions. Due to its intense color, **1** was also investigated by UV-Vis spectroscopy in the solid state. The onset of a broad absorption is observed below 800 nm which continues to the UV-region thus indicating the superposition of several absorption bands (Fig. 3).

From the absorption spectrum of **1**, the HOMO–LUMO gap was determined as 1.56 eV (795 nm, Fig. 3). Surprisingly, the band gap is smaller compared with the largest binary copper sulfide cluster [$Cu_{136}S_{56}(SCH_2C_4H_3O)_{24}$(dpppt)$_{10}$] (1.87 eV, 664 nm).[3f] However, due to quantum confinement effects, the band gap is still larger compared to band gaps of different copper(I) sulfide phases like *e.g.* chalcocite (1.2 eV)[11] or dijurleite (1.3 eV).[12]

In summary, we have prepared and fully characterized the second largest binary copper sulphide nanocluster [$Cu_{52}S_{12}(SCH_2C_6H_4{}^{t}Bu)_{28}(PPh_3)_8$] (**1**), which was reproducibly obtained from the reaction of [CuSCH$_2$C$_6$H$_4$^{t}Bu] and S(SiMe$_3$)$_2$ in the presence of triphenylphosphine. Hence, this synthesis demonstrates an easy approach towards small and size-homogeneous copper sulfide nanoparticles. The intensely red-colored compound was structurally analysed by single crystal X-ray diffraction as well as different spectroscopic techniques. Compound **1** represents a ligand-protected Cu_2S nanoparticle with a spherical shape and diameters between 2.2 nm and 3 nm. Cluster **1** features a distorted fcc packed Cu-substructure and forms a hcp throughout the crystal lattice. According to UV-Vis spectra, the band gap of **1** was found to be 1.56 eV, which is larger compared with different copper(I) sulfide phases.

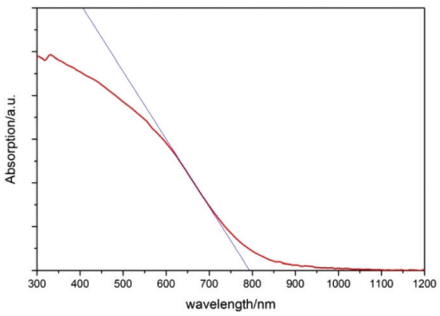

Fig. 3 UV-Vis spectrum of **1** (red) and tangent line (blue) to determine the HOMO–LUMO gap (red).

Notes and references

‡Synthesis of [$Cu_{52}S_{12}(SCH_2C_6H_4{}^{t}Bu)_{28}(PPh_3)_8$] **1**: the copper(I) thiolate [CuSCH$_2$C$_6$H$_4$^{t}Bu] (450 mg, 1.85 mmol, 1.00 eq.) and triphenylphosphine (375 mg, 1.43 mmol, 0.77 eq.) are suspended in toluene (25 mL) and stirred for 5 minutes at room temperature. S(SiMe$_3$)$_2$ (0.08 mL, 68 mg, 0.38 mmol, 0.20 eq.) is added with a syringe. Within two hours, a color change from yellow to dark red is observed and a clear solution is obtained. After 24 hours of stirring, the solvent is removed under vacuum and *n*-heptane (35 mL) is added. A brownish precipitate forms, which is subsequently removed by filtration to afford a dark red solution, which is stored at room temperature for two days. Red crystals are formed at the wall of the Schlenk-tube. These are separated from the mother liquor by decantation. The crystals are washed with *n*-pentane (3 × 15 mL) and finally dried under high vacuum. Yield: 105 mg (32% with respect to the limiting reagent S(SiMe$_3$)$_2$). IR (ATR): $\tilde{\nu}$ (cm^{-1}) = 3051 (m), 2956 (vs), 2903 (m), 2866 (m), 1510 (m), 1475 (m), 1432 (m), 1361 (m), 1267 (vw), 1229 (m), 1199 (w), 1099 (m), 1020 (w), 876 (w), 828 (w), 742 (m), 692 (s), 551 (w), 515 (m), 429 (vw). Elemental analysis calcd. (%) for [$C_{452}H_{540}Cu_{52}P_8S_{40}$ × 3 C_7H_{14}] (10807.87): C 51.17, H 5.28, S 11.55; found C 51.74, H 5.06, S 11.51.

§Crystal data for **1**·10*n*-heptane: [$C_{522}H_{700}Cu_{52}P_8S_{40}$] ($M$ = 11 809.02 g mol^{-1}): monoclinic, space group $C2/c$ (no. 15), a = 41.0006(8) Å, b = 31.9188(4) Å, c = 45.9429(9) Å, β = 113.674(1)°, V = 55 065(2) Å^3, Z = 4, T = 150.15 K, μ(CuKα) = 4.080 mm^{-1}, D_{calc} = 1.424 g cm^{-3}, 147 112 reflections measured (4.89° ≤ 2Θ ≤ 120.606°), 39 955 unique (R_{int} = 0.088, R_{sigma} = 0.103) which were used in all calculations. The final R_1 was 0.051 ($I > 2\sigma(I)$) and wR_2 was 0.126 (all data).

1 (*a*) Y. Yin and A. P. Alivisatos, *Nature*, 2005, **437**, 664; (*b*) A. N. Goldstein, C. M. Echer and A. P. Alivisatos, *Science*, 1992, **256**, 1425; (*c*) A. P. Alivisatos, *Science*, 1996, **271**, 933; (*d*) Y. Volokitin, J. Sinzig, L. J. de Jongh, G. Schmid, M. N. Vargaftik and I. I. Moiseevi, *Nature*, 1996, **384**, 621;

(*e*) R. Langer, M. Yadav, B. Weinert, D. Fenske and O. Fuhr, *Eur. J. Inorg. Chem.*, 2013, 3623; (*f*) P.-C. Chen, Y.-C. Li, J.-Y. Ma, J.-Y. Huang, C.-F. Chen and H.-T. Chang, *Sci. Rep.*, 2016, **6**, 24882; (*g*) P. V. V. N. Kishore, J.-H. Liao, H.-N. Hou, Y.-R. Lin and C. W. Liu, *Inorg. Chem.*, 2016, **55**, 3663; (*h*) C. W. Liu, B. Sarkar, Y.-J. Huang, P.-K. Liao, J.-C. Wang, J.-Y. Saillard and S. Kahlal, *J. Am. Chem. Soc.*, 2009, **131**, 11222; (*i*) R. S. Dhayal, J.-H. Liao, H.-N. Hou, R. Ervilita, P.-K. Liao and C. W. Liu, *Dalton Trans.*, 2015, **44**, 5898.

2 (*a*) O. Fuhr, S. Dehnen and D. Fenske, *Chem. Soc. Rev.*, 2013, **42**, 1871; (*b*) S. Dehnen and D. Fenske, *Chem. – Eur. J.*, 1996, **2**, 1407.

3 (*a*) J. F. Corrigan, O. Fuhr and D. Fenske, *Adv. Mater.*, 2009, **21**, 1867; (*b*) A. Eichhöfer, J. F. Corrigan, D. Fenske and E. Tröster, *Z. Anorg. Allg. Chem.*, 2000, **626**, 338; (*c*) S. Dehnen, D. Fenske and A. C. Deveson, *J. Cluster Sci.*, 1996, **7**, 351; (*d*) C. B. Khadka, B. K. Najafabadi, M. Hesari, M. S. Workentin and J. F. Corrigan, *Inorg. Chem.*, 2013, **52**, 6798; (*e*) S. Ahmar, D. G. MacDonald, N. Vijayaratnam, T. L. Battista, M. S. Workentin and J. F. Corrigan, *Angew. Chem., Int. Ed.*, 2010, **49**, 4422; (*f*) M.-L. Fu, I. Issac, D. Fenske and O. Fuhr, *Angew. Chem., Int. Ed.*, 2010, **49**, 6899.

4 (*a*) C. E. Anson, A. Eichhöfer, I. Issac, D. Fenske, O. Fuhr, P. Sevillano, C. Persau, D. Stalke and J. Zhang, *Angew. Chem., Int. Ed.*, 2008, **47**, 1326; (*b*) S. Bestgen, X. Yang, I. Issac, O. Fuhr, P. W. Roesky and D. Fenske, *Chem. – Eur. J.*, 2016, **22**, 9933; (*c*) Y. Liu, B. Khalili Najafabadi, M. Azizpoor Fard and J. F. Corrigan, *Angew. Chem., Int. Ed.*, 2015, **127**, 4914.

5 (*a*) X. Yang, I. Isaac, C. Persau, R. Ahlrichs, O. Fuhr and D. Fenske, *Inorg. Chim. Acta*, 2014, **421**, 233; (*b*) B. Hu, C.-Y. Su, D. Fenske and O. Fuhr, *Inorg. Chim. Acta*, 2014, **419**, 118; (*c*) B. Khalili Najafabadi and J. F. Corrigan, *Dalton Trans.*, 2014, **43**, 2104.

6 L. M. Nguyen, M. E. Dellinger, J. T. Lee, R. A. Quinlan, A. L. Rheingold and R. D. Pike, *Inorg. Chim. Acta*, 2005, **358**, 1331.

7 (*a*) H. T. Evans, *Science*, 1979, **203**, 356; (*b*) H. T. Evans, *Z. Kristallogr.*, 1979, **150**, 299; (*c*) P. Rahlfs, *Z. Phys. Chem., Abt. B*, 1936, **31**, 157.

8 K. Tang, T. Xia, X. Jin and Y. Tang, *Polyhedron*, 1993, **12**, 2895.

9 (*a*) S. Dehnen, A. Schäfer, R. Ahlrichs and D. Fenske, *Chem. – Eur. J.*, 1996, **2**, 429; (*b*) S. Sculfort and P. Braunstein, *Chem. Soc. Rev.*, 2011, **40**, 2741; (*c*) S. Dehnen, A. Schäfer, D. Fenske and R. Ahlrichs, *Angew. Chem.*, 1994, **106**, 786.

10 (*a*) S. Schneider, J. A. Roberts, M. R. Salata and T. J. Marks, *Angew. Chem., Int. Ed.*, 2006, **45**, 1733; (*b*) T.-A. D. Nguyen, Z. R. Jones, B. R. Goldsmith, W. R. Buratto, G. Wu, S. L. Scott and T. W. Hayton, *J. Am. Chem. Soc.*, 2015, **137**, 13319.

11 L. D. Partain, P. S. McLeod, J. A. Duisman, T. M. Peterson, D. E. Sawyer and C. S. Dean, *J. Appl. Phys.*, 1983, **54**, 6708.

12 O. Madelung, *Semiconductors: data handbook*, Springer, 3. Auflage, Berlin, 2004.